MDPI

Article

Characterization of Extracellular Polymeric Substances Produced by an *Acidianus* Species and Their Relevance to Bioleaching

Camila Castro [1,*], Edgardo R. Donati [1] and Mario Vera [2]

1 CINDEFI (CCT La Plata—CONICET, U.N.L.P.), Facultad de Ciencias Exactas, Universidad Nacional de La Plata, La Plata 1900, Argentina
2 Institute for Biological and Medical Engineering, Schools of Engineering, Biological Sciences and Medicine, Pontificia Universidad Católica de Chile, Santiago 4860, Chile
* Correspondence: castro.camila@biotec.quimica.unlp.edu.ar

Abstract: Extracellular polymeric substances (EPS) produced by microorganisms play a crucial role in various bioprocesses, including bioleaching. The microbial leaching of metal sulfides requires an initial cell attachment, which is facilitated by EPS. These substances are mixtures of polysaccharides, proteins, lipids, and other compounds, and their composition and properties can vary depending on the species, growth conditions, and environmental factors. Despite the significance of iron/sulfur oxidizing species in biomining processes, the knowledge of the interfacial processes between thermoacidophilic archaeal species and mineral surfaces is limited. This study examines the cell surface characteristics and EPS produced by an *Acidianus* strain. The research was conducted using microscopic techniques, Zeta-potential measurements, spectrophotometric methods, Fourier transform infrared spectroscopy, and fluorescence lectin-binding analysis. The results suggest that non-soluble substrates, such as sulfur or pyrite, induce changes in cell surface structures, including the presence of cell appendages, wider cell envelopes, higher hydrophobicities, and increased EPS production, compared to cells grown with soluble substrates such as tetrathionate or ferrous iron. The EPS mainly consist of proteins and carbohydrates, including glucose, manose, *N*-acetylgalactosamine, and *N*-acetylglucosamine residues. This study contributes to a better understanding of the relationship between thermophilic archaea and mineral surfaces in biomining processes.

Keywords: archaea; extracellular polymeric substances; cell surface; thermophiles; bioleaching

1. Introduction

Biomining is a worldwide applied biotechnology for mineral processing and metal extraction from ores and concentrates. The mobilization of metals from insoluble ores can occur spontaneously in nature, causing acid mine/rock drainage (AMD/ARD). For the dissolution of metal sulfides an oxidizing agent and an acidic environment are required to maintain metal cations in solution. This condition can be provided by acidophilic iron- and sulfur oxidizing microorganisms; these can oxidize ferrous iron and/or reduced inorganic sulfur compounds (RISCs), producing ferric iron (oxidizing agent) and sulfuric acid [1].

Microbial leaching of metal sulfides requires an initial cell attachment, which contributes to initiate metal dissolution. Several laboratory studies have demonstrated that the electrochemical process resulting in the dissolution of sulfide minerals takes place at the interface between the microbial cell and the mineral surface [2]. It is well known that extracellular polymeric substances (EPS) mediate the contact between cell/surface. EPS is, in most cases, produced as a capsule surrounding the cell surface and contributes to the adhesion to certain surfaces or cell aggregates when forming biofilms. Other EPS functions are provision of a protective barrier, water retention, sorption of organic compounds and

inorganic anions, hosting enzyme activities, and contributing to genetic exchange mechanisms and cell to cell communication processes by providing microenvironments where these processes can occur. The EPS matrix is formed by different compounds secreted by microbes, release of cellular material/products by cell lysis, as well as organic or inorganic matter sequestered from the medium [3]. The EPS usually consist of polysaccharides, proteins, lipids, and DNA. However, microorganisms change their composition according to electron donors and the presence of surface and cell–cell communication processes.

There are several iron/sulfur oxidizing species relevant to biomining processes. The main bioleaching genera among the mesophiles are *Acidithiobacillus*, *Leptospirillum*, *Acidiphilium*, *Sulfobacillus*, and *Ferrimicrobium*; whereas Archaeal genus, such as *Acidianus*, *Sulfolobus*, *Sulfuracidifex*, and *Metallosphaera*, are thermo-acidophiles frequently found in geothermal areas and bioleaching operations at high temperatures [4]. The archaeal tolerance to the extreme environmental conditions (low pH, high temperatures and concentrations of metal ions) and their physicochemical characteristics have been largely attributed to the particular structure of the cell envelope [5].

The understanding of biofilm formation by metal-oxidizing microorganisms is of great importance in influencing mineral dissolution rates and preventing acid mine drainage (AMD) [6]. To date, detailed knowledge of interfacial processes between archaeal cells and mineral surfaces is still rather limited. Archaeal cell surface properties, EPS composition, amounts, and chemical characteristics are largely unresolved areas of research. These are relevant factors to understand their function in bioleaching processes. In order to obtain improved data on these points, we studied the cell surface characteristics and EPS produced by the thermoacidophilic Archaeal strain *Acidianus copahuensis* DSM 29038 cultured with different energy substrates. This thermoacidophilic archaea strain belongs to the *Sulfolobales* order and has been reported and isolated from the volcanic geothermal area of Copahue at Neuquén province in Argentina [7]. *A. copahuensis* shows a great physiological flexibility by growing on sulfur, tetrathionate, ferrous iron, and glucose under aerobic conditions; but it can also develop under anaerobic conditions using sulfur or hydrogen as electron donors and ferric iron or sulfur as electron acceptors. It grows in a temperature range of 55 °C to 80 °C and pH range from 1 to 5, with optimum conditions at 75 °C and pH 3. Additionally, *A. copahuensis* has been shown to contain multiple mechanisms of tolerance and resistance to heavy metals and metalloids and acid tolerance, including proton pumps and efficient repair systems for damaged proteins [8]. *A. copahuensis* was successfully employed to recover metals such as copper and zinc from low-grade and refractory ores [9–11]. The metabolic versatility of this strain also makes it a valuable tool for exploring the interactions between energy metabolism and extreme environments. Further study of this organism will expand our understanding of the diversity and resilience of life in extreme environments and contribute to the development of new and more efficient biotechnology applications.

2. Materials and Methods

2.1. Microorganisms and Cultivation

A. copahuensis DSM 29038 [7] was cultivated in flasks containing Mackintosh basal salt solution (MAC) [12] at pH 2. The medium was sterilized by autoclaving for 20 min. The basal medium was supplemented with either 10 g/L elemental sulfur ($S°$) powder, 3 g/L potassium tetrathionate ($K_2S_4O_6$), 6 g/L ferrous iron as $FeSO_4 \cdot 7H_2O$, 1% (*w/v*) pyrite, 1 g/L glucose, and/or 1 g/L yeast extract as energy sources. Flasks were incubated aerobically at 65 °C, with shaking at 120 rpm.

2.2. Cell Surface Characterization

2.2.1. Hydrophobicity

Cultures in the stationary phase were filtered, and cells were harvested by centrifugation at $5800 \times g$ for 10 min. Cell pellets were washed twice with MAC solution and then resuspended to an OD_{400} of 0.3–0.4 (A_0) in PUM buffer (19.7 g/L K_2HPO_4, 7.26 g/L KH_2PO_4, 1.8 g/L H_2NCONH_2, 0.2 g/L $MgSO_4 \cdot 7H_2O$, pH 7). To 1.2 mL of cell suspension,

0.2 mL of chloroform or *n*-hexadecane was added, and samples were vortexed for 90 s. The mixtures were allowed to settle during 15 min, to allow complete phase separations. Subsequently, samples of aqueous phases were removed to measure the OD$_{400}$ (A_t). The percentage of cell partition to the different solvents was calculated as $(1 - A_t/A_0) \times 100$. In addition, these results were verified by performing cell counts of the aqueous phases before and after solvent treatment. Each test was conducted in triplicate.

2.2.2. Zeta Potential Determinations

Electrophoretic mobilities of *A. copahuensis* cells grown in different conditions were measured using a Brookhaven 90 Plus/Bi-MAS instrument. Cells were prepared by harvesting, as previously described, and resuspended in fresh MAC solution. Measurements were conducted at different pH values (within a range of 2 to 7) using cell suspensions of 1×10^8 cells/mL.

2.2.3. Scanning and Transmission Electron Microscopy (SEM/TEM)

A. copahuensis cells grown in different conditions were fixed with 2.5% glutaraldehyde (pH 7.2) at 4 °C for 1 h, post-fixed with 2% osmium tetroxide, and dehydrated in a graded series of alcohol (25%−100%). Dehydrated samples were dried in a critical point chamber and afterwards coated with a thin layer of gold and visualized by a LEO EVO 40 XVP scanning electron microscope (SEM).

Microbial ultra-structures and morphological characteristics of *A. copahuensis* were studied by transmission electron microscopy (TEM) (JEOL JEM 1200EX II TEM). *A. copahuensis* cells grown in different conditions were harvested by centrifugation at $5800 \times g$ for 10 min, and cell pellets were washed twice with MAC solution. For TEM visualization, cells were prepared as described above and then embedded in Spur resin and cut with an ultramicrotome (Supernova, Reichert-Jung). Thin sections were stained with uranyl acetate. Fixed samples (without post fixation and dehydrations) were negatively stained with uranyl acetate and visualized by TEM.

2.3. EPS Extraction

Capsular EPS were extracted using a cation exchange resin (CER) (DOWEX Marathon C, Sigma, St. Louis, MO, USA) as previously described [13]. Suspensions containing extracted EPS were dialyzed to eliminate metabolites and salts of low molecular weight, using cellulose dialysis membranes with a 3.5 KDa cut-off (SnakeSkin™, Thermo Scientific™, Waltham, MA, USA) in 5 L of ultra-pure water for 24 h at 4 °C. The total amount of extracted EPS was measured by dry weight after lyophilization. All EPS extractions were conducted in duplicate.

2.4. Characterization of EPS
2.4.1. Biochemical Analyses

The major components of EPS were quantified separately by chemical colorimetric methods. All chemical analyses were carried out at least in triplicate for each determined parameter, using chemicals of analytical grade. Polysaccharides were quantified by the phenol-sulfuric acid method [14], using glucose standards. The protein content was analyzed using the Bradford method [15] using bovine albumin serum as a standard. Uronic acid levels were determined as described in [16] using D-glucuronic acid as a standard. Concentrations of humic-like substances were calculated by a modified Lowry protocol [17] using humic compound as a standard. Nucleic acid content was determined using a NanoDrop™ 2000c (Thermo Scientific™, Waltham, MA, USA).

2.4.2. Fourier Transform Infrared (FTIR) Spectroscopy

FTIR was used to determine the variation in the chemical groups in the EPS due to different growth conditions. One milligram of freeze-dried EPS was mixed with KBr to

form a pellet. The infrared spectra were recorded using a spectrum Bruker IFS 66 in the region between 300 cm^{-1} and 4000 cm^{-1}.

2.4.3. Fluorescence Lectin-Binding Assays (FLBA)

Planktonic cells with different history substrate were filtered on autoclaved polycarbonate filters (GTTB, θ2.5 cm, 0.2 μm pore size, Millipore®, Burlington, MA, USA). Planktonic cells on filters or sessile cells on pyrite coupons were stained by 4',6-diamidino-2-phenylindole (DAPI). Stained samples were washed twice with filter-sterilized tap water. Then, samples were covered with solutions of fluorescently labeled lectins (Invitrogen, Waltham, MA, USA) with different moiety specificities following the manufacturer instructions. Stained samples were washed three times with filter-sterilized tap water to remove unbound lectins. Finally, samples were dried at room temperature and mounted on glass slides using an anti-fading agent to prolong the fluorescence of the dyes. Samples were visualized by epifluorescence microscopy (EFM) (Axiovert−100 MBP microscope, Zeiss, Jena, Germany).

2.5. Bioleaching Tests

Bioleaching assays were performed in Erlenmeyer flasks, each containing 50 mL MAC solution (pH 2) and 1% *w/v* of sterile pyrite (50–100 mesh). Flasks were inoculated with 5×10^8 cells/mL, using *A. copahuensis* cells pregrown with sulfur, ferrous iron, or pyrite as an energy source. Flasks were incubated at 65 °C with shaking at 120 rpm. Samples of 1 mL were taken periodically from supernatants, and pH, ferric and ferrous iron were determined by the *o*-phenanthroline method [18].

3. Results and Discussion

3.1. Cell Morphology

To gain further insights into *A. copahuensis* cell morphology, cells grown with different substrates were analyzed by microscopy techniques (Figure 1). EPS production was visualized in cells grown with soluble and non-soluble substrates. SEM micrographs show the presence of EPS on the cell surface and also connecting cells (Figure 1e,f). In addition, EPS displayed in TEM micrographs as a diffuse material surrounding individual cells and groups of cells (Figure 1a–d). *A. copahuensis* cells grown with different substrates were similar in size and displayed a pleomorphic shape with slightly variable dimensions, and they presented a typical archaeal cell envelope formed by a single membrane and covered by a paracrystalline glycoprotein layer (S-layer) [7,10]. It has also been reported that *A. copahuensis* cells are covered by capsules, but they differ in thickness and appearance according to the culture condition [10].

Further TEM examinations revealed the presence of intracellular dark structures (Figure 1b). Some cells also exhibited numerous cytoplasmic inclusions. These dark structures were exclusively detected when cells were cultured with elemental sulfur or tetrathionate. Similar ultrastructures were identified as polyphosphate (polyP) granules in some archaeal strains, such as *Sulfolobus* spp., *Archaeaglobus fulgidus*, and *Methanospirillum hungatei* and in members of *Methanosarcinaceae* [19–21]. In extremophilic archaea, polyP are involved in diverse physiological functions, such as metal resistance, salt tolerance, adaptation to oxidative stress, temperature tolerance, and other environmental stresses [22]. In addition, TEM studies demonstrated that the hyperthermophilic archaeal *Thermococcus* species produced sulfur vesicles similar to these dark structures found in *A. copahuensis* [23]. Several bacteria also form extracellular and/or intracellular sulfur reserves, usually in the form of sulfur globules. The structure, chemical composition, and metabolic pathways related to sulfur globule formation and degradation differ between species [24]. In some microorganisms, these reserves are transient and completely degraded after oxidation of the sulfur available, thus providing energy storage compounds [25]. In others, sulfur globules serve to remove excess toxic compounds, in sulfur-detoxifying function [26]. We suspect that in *A. copahuensis* these structures may accumulate excess sulfur within the cells

to be used during substrate starvation conditions. However, further studies are necessary to confirm the nature and function of these structures.
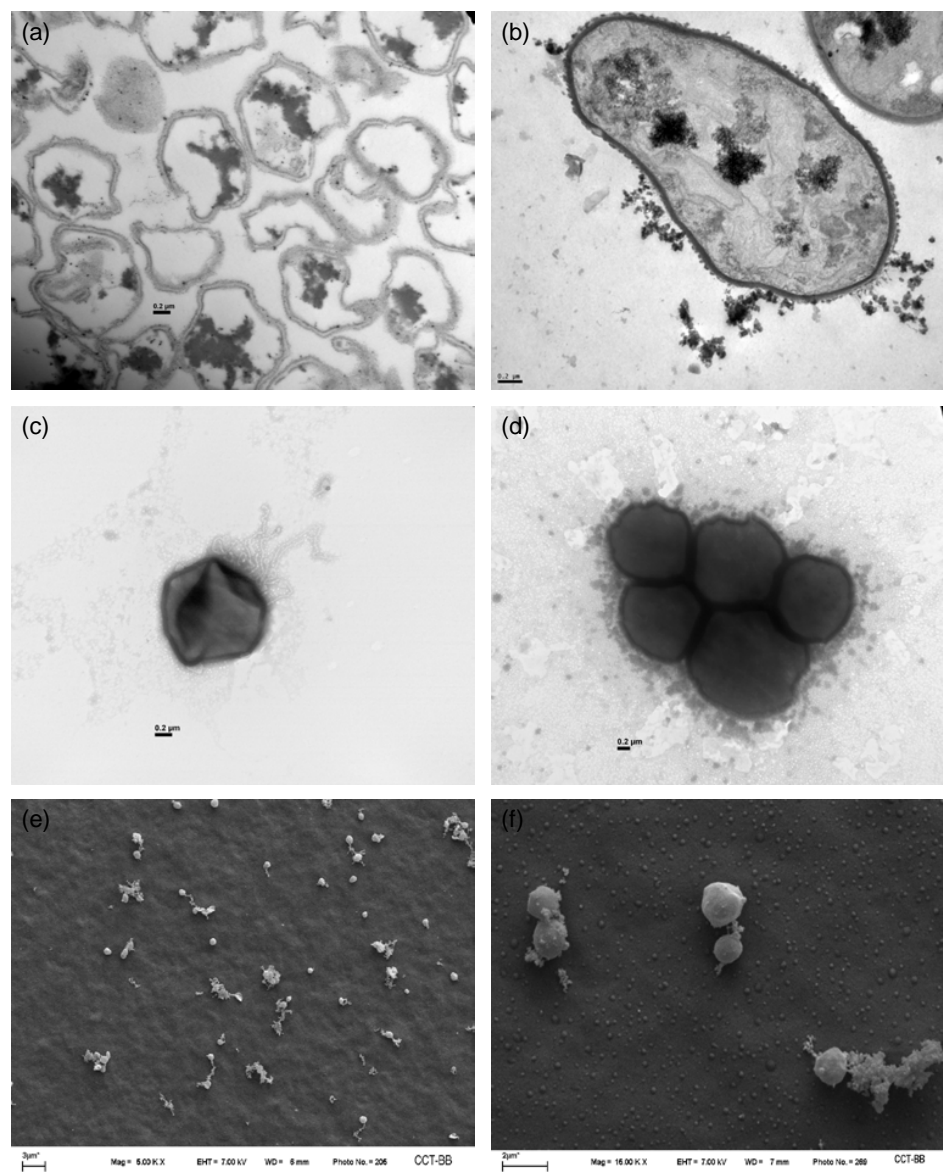

Figure 1. *A. copahuensis* cells visualized by transmission electron microscopy (**a–d**) and scanning electron microscopy (**e,f**) micrographs. Cells were grown with tetrathionate (**a,e**), sulfur (**b,c**), glucose (**d**), and pyrite (**f**).

Negative staining micrographs revealed the presence of extracellular appendages when cells were grown with non-soluble substrates such as pyrite or sulfur (autotrophic and mixotrophic conditions) (Figure 1c). The substrate nature seems to affect the production of these cellular structures, since appendages were not detected when cells were grown with soluble substrates such as tetrathionate or glucose. On account of this, the function of these surface structures may be involved in cell attachment to the solid substrate. Several types of cell surface structures were reported in archaeal species; some of them are also present in bacteria but other appendages such as hami, cannulae, bindosome, and archaellum are archaeon-specific structures [27–29]. Most surface structures are involved in cellular attachment to surfaces, maintaining cell–cell contact, communication, exchange of nutrients and genetic material, and motility [29,30]. Among *Sulfolabales*, some *Sulfolubus* and *Metallosphaera* strains appear to possess cell surface appendages [31]. Zolghadr and

colleagues [32] demonstrated that flagella and UV-induced pili are essential for the initial attachment of *Sulfolobus solfataricus* to different surfaces.

3.2. Cell Surface Characterization

The solvent affinity of *A. copahuensis* cells to chloroform and *n*-hexadecane was studied. Figure 2 shows the adhesion percentages of *A. copahuensis* cells grown under different conditions to both solvents mentioned above. The affinities of *A. copahuensis* to both tested solvents were low; even the adhesion percentages to *n*-hexadecane were nearly null in most metabolic conditions. These results suggest a hydrophilic cell surface character for the studied thermoacidophilic archaeal species. In the same way, low hydrophobicity percentages were found in other archaeal species, such as *Metallosphaera sedula*, *A. manzaensis,* and *Acidianus* sp. [33–35]. Chloroform and *n*-hexadecane are solvents with different polarities and physical properties, which may influence cells' affinity for them. Chloroform is a polar solvent with a molecular structure that allows it to form hydrogen bonds and Van der Waals forces with polar molecules. In contrast, *n*-hexadecane is a more hydrophobic and non-polar solvent than chloroform. On the other hand, cells are mainly composed of polar molecules such as proteins, carbohydrates, and nucleic acids. Therefore, they have a natural tendency to interact with polar solvents such as chloroform. As a result, cells may have a higher affinity for chloroform due to these molecular interactions.
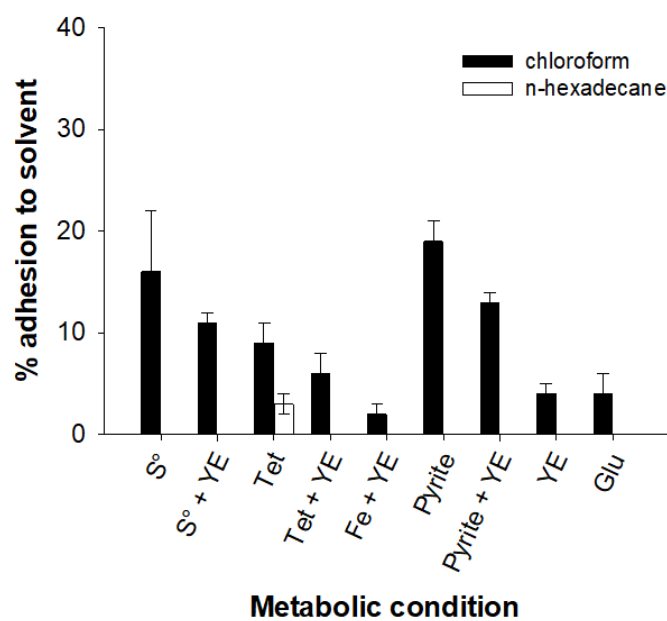

Figure 2. Adhesion percentages of *A. copahuensis* to chloroform and *n*-hexadecane, cultured in nine different growth conditions: elemental sulfur (S°), elemental sulfur and yeast extract (S° + YE), potassium tetrathionate (Tet), potassium tetrathionate and yeast extract (Tet + YE), ferrous iron and yeast extract (Fe + YE), pyrite, pyrite and yeast extract (Pyrite + YE), yeast extract (YE), and glucose (Glu). Error bars show standard deviation from three independent experiments ($n = 3$).

The affinity of *A. copahuensis* cells for chloroform showed variations according to the growth conditions. Results indicated that cells grown with non-soluble substrates (sulfur or pyrite) were more hydrophobic than cells grown on soluble substrates (tetrathionate, ferrous iron, yeast extract, or glucose). Both pyrite and sulfur have been reported to be hydrophobic under conditions similar to those used in this study [36,37]. This suggests that hydrophobic interactions may be relevant in the adhesion of *A. copahuensis* cells to these substrates. It is presumable that cells grown on insoluble substrates develop an outer layer of hydrophobic molecules, such as adhesion proteins and lipids, to adhere to the surface of the substrate. This hydrophobic layer may also help protect the cells from unfavorable environmental conditions, such as the presence of metals, toxic substances, and oxidative

stress generated by pyrite leaching [38]. In contrast, cells grown on soluble substrates do not need to develop this hydrophobic layer and may therefore be less hydrophobic. However, when microorganisms use pyrite or sulfur as an energy source, they can produce polymers and other substances that modify the hydrophobicity of the substrate surface [39,40]. As a consequence, the surface properties of pyrite and elemental sulfur may be influenced by the presence of microorganisms or by the adsorption of organic or inorganic substances present in the environment, which could alter their hydrophobicity and charge. Similar trends were observed in studies carried out with other iron/sulfur-oxidizing microbial species [33,34,41,42]. He and colleagues [34] concluded that the hydrophobicity of solid substrate-grown cells of *A. manzaensis* may help microorganisms to adhere onto the substrate and facilitate it becoming an energy source. The results suggest that the source of energy used by the cells may have an impact on their hydrophobicity and that cells grown on insoluble substrates may be more hydrophobic than those grown on soluble substrates.

Zeta potential measurements were performed on *A. copahuensis* cells grown with the aforementioned energy sources. The zeta potential value of cells is related to the presence of functional groups, such as amino and carboxyl groups on the cell surface components, which can be ionized depending on the pH of the medium. The isoelectric points (IEP) and zeta potential values at the optimum growth pH for this archaeon are shown in Table 1. In all tested conditions, measurements revealed that *A. copahuensis* cells exhibited a net positive charge below pH 3, above which the superficial cell charge is strongly affected (data not shown). These results agree with studies reported earlier for *Acidithiobacillus ferrooxidans*, *Acidithiobacillus thiooxidans*, *Acidithiobacillus caldus*, *Metallosphaera hakonensis*, and *A. manzaensis* [33,34,42–45]. It is well known that zeta potential values can vary depending on sample-specific conditions, such as purity and crystalline structure, as well as the composition and ionic strength of the solution in which they are found, but negative zeta potential values have been reported for both sulfur and pyrite at pH 2 [41,46,47]. Therefore, it is expected that cells grown on sulfur or pyrite would exhibit higher positive zeta potential values, which could promote cell adhesion to the substrate through electrostatic interactions between the positive charges of the cell surface and the negative charges of the substrate. *A. copahuesis* grown with glucose had the lowest IEP (3), whereas cells grown with sulfur, tetrathionate, ferrous iron, pyrite, and/or yeast extract as energy sources exhibited IEPs of 4 to 6. The observed differences between IEPs of cells cultured with different substrates could be attributed to the presence of different types and amounts of functional groups over the cell surface, which influences the cell charge. Previous studies have shown that IEP values between 2.0 and 2.8 indicate a predominance of glucuronic acids or polysaccharides negatively charged (carboxyls, phosphates, and sulfates groups); however, IEP values greater than 3.0 are difficult to interpret because they may reflect mixed contributions of proteins and/or polysaccharides [45,48]. Based on the obtained IEP values for most of the studied conditions, it cannot be conclusively determined which type of biopolymer predominates on the cell surface of *A. copahuensis*. An exception to this was observed when cells were grown with glucose, which could include considerable amounts of glucuronic acids and/or other negatively charged polysaccharides.

Table 1. Zeta potential measurements at pH 2 and IEP values of *A. copahuensis* cultured in different growth conditions.

Growth Condition	Zeta Potential at pH 2 (mV)	IEP
S°	19 ± 4	5.2
S° + YE	7 ± 2	4.1
Tet	11 ± 2	4.5
Tet + YE	14 ± 1	4.4
Fe + YE	6 ± 1	4.2
Pyrite	15 ± 1	5.5
Pyrite + YE	11 ± 1	6.0
YE	2 ± 1	4.0
Glu	7 ± 2	3.1

3.3. EPS Production and Characterization

Figure 3 shows the capsular EPS extracted from *A. copahuensis* cells cultured with different energy sources. Cells cultured heterotrophically (glucose or yeast extract) and autotrophically with tetrathionate as an energy source displayed comparable amounts of EPS production (between 0.02 and 0.03 pg-EPS/cell). Under mixotrophic conditions (with tetrathionate and yeast extract), the EPS production was 0.11 pg-EPS/cell. The maximum EPS yield was achieved by planktonic cells cultured with pyrite (0.28 pg-EPS/cell), reaching a two-fold increase of EPS production compared with the rest of the analyzed conditions. Zhang et al. [35,49] found that both capsular and colloidal EPS production in *Acidianus* sp. is enhanced by non-soluble substrates such as pyrite and sulfur as compared to soluble substrates such as iron and tetrathionate, respectively. It is well known that the microbial adhesion process on the mineral surface is mediated by the EPS produced by cells; and the adhesion and/or contact with the solid surface stimulate the EPS production [2,50]. When pyrite is the only substrate, *A. copahuensis* may produce more EPS to become absorbed on the mineral to obtain energy from the available substrate. EPS plays a major role in the oxidation of metal sulfides. The electrochemical processes leading to the dissolution of metal sulfides, such as pyrite, take place at the interface between the microbial cell and the surface of the sulfide mineral, and this space is filled by EPS. These substances could act by concentrating ferric ions that oxidize the metal sulfide, thus releasing ferrous ions, sulfur, and RISCs that can be used as an energy source by acidophilic microorganisms [2,51,52]. The importance of EPS in adhesion was highlighted by the findings of Yu et al. [53], who conducted a study to investigate the effect of EPS on the adhesion of *A. ferrooxidans* to pyrite and chalcopyrite surfaces. The study found that adhesion accelerated mineral leaching and that the extraction of the EPS layer from cells resulted in the inhibition of cell adhesion.
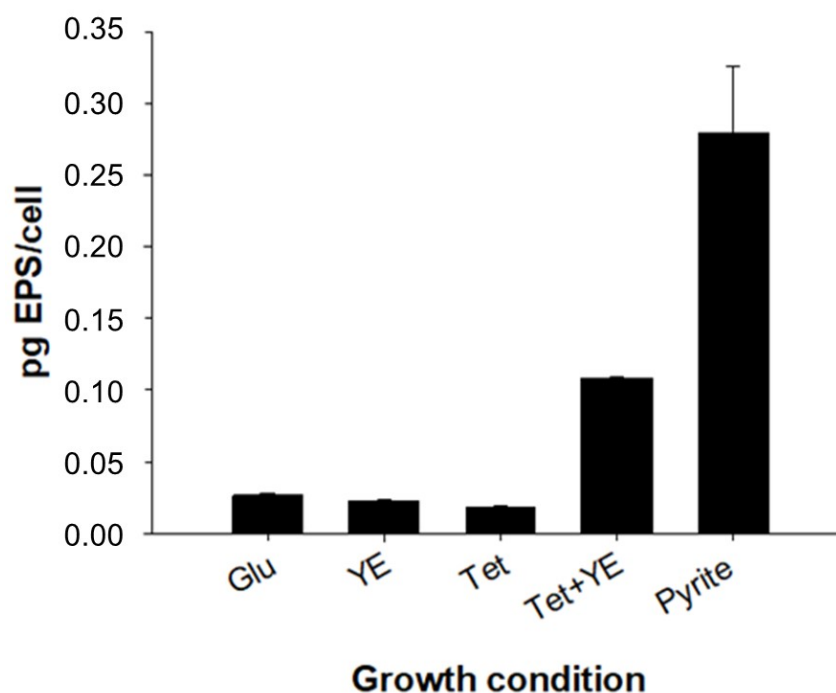

Figure 3. Comparison of capsular EPS produced per cell of *A. copahuensis* cells cultured in different growth conditions: glucose (Glu), yeast extract (YE), tetrathionate (Tet), tetrathionate and yeast extract (Tet + YE), and pyrite. Error bars show standard deviation from two independent experiments (n = 2).

Table 2 shows the compounds detected in EPS produced by *A. copahuensis* grown under different conditions. Our results demonstrated that EPS produced by *A. copahuensis* were composed of polysaccharides, proteins, uronic acids, and humic-like substances. However, a large proportion of compounds forming part of the EPS could not be identified, except in

EPSs produced by cells grown in glucose, in which about 65% of the compounds present could be identified. The type and proportion of each constituent were variable according to the growth condition of the cells. The low or null levels of DNA in the extracted EPS indicated there was no significant contamination by cell lysis during the extraction.

Table 2. Composition of EPS (mg/g-DW of EPS) produced by *A. copahuensis* grown under different conditions.

Growth Condition	Proteins	Carbohydrates	Uronic Acids	Humic-Like Substances	Nucleic Acids
Glu	66 ± 3	580 ± 80	70 ± 10	38 ± 1	BDL
YE	105 ± 5	52 ± 9	40 ± 2	130 ± 5	BDL
Tet + YE	61.2 ± 0.5	26 ± 7	27 ± 1	100 ± 4	0.6 ± 0.3
Tet	10.0 ± 0.5	BDL	33 ± 1	19 ± 3	BDL
Pyrite (planktonic cells)	18 ± 1	91 ± 20	29 ± 2	19 ± 4	BDL
Pyrite (sessile cells)	6 ± 1	37 ± 10	27 ± 8	14 ± 4	BDL

BDL: Below detection limit.

Among the EPS fractions, the protein content was in a range of 6 mg/g-DW to 105 mg/g-DW, and proteins were found to be the main components identified in EPS produced by cells grown with yeast extract and tetrathionate with and without yeast extract. Govender and Gericke [54] analyzed the composition of EPS produced from mixed biofilms (using various mineral resources) of mesophiles, moderate thermophiles, and extreme thermophiles. They recorded higher levels of proteins in the extreme thermophile system composed of *Acidianus* sp., *Sulfolobus* sp., and *Metallosphaera* sp. as compared with those protein levels measured in mesophile and moderate thermophile ones. These results could be explained by the involvement of several proteins in metabolic processes, such as activation and transportation of sulfur compounds for their cytoplasmic oxidation, and iron oxidation. In addition, proteins may have a structural function, participating in the adhesion and biofilm formation process.

Uronic acids were detected in all EPS fractions. Uronic acids are replicate units of acidic polysaccharides or mucopolysaccharides. These anionic polymers could stimulate bioflocculation, ion exchange, and accumulation of toxic metals [55,56]. They also can bind metal cations [57]. Bioflotation studies performed with microbial EPS suggested that EPS rich in acidic polysaccharides produced by the thermoacidophilic archaeal consortium result in higher recoveries of chalcopyrite [54].

Humic-like substances were also detected in all EPS fractions. The important properties of humic-like substances were reported to be adhesion, as well as being electron donors or acceptors, with minor roles in flocculation and biosorption of EPS [3,58].

Significant differences were found in relation to polysaccharide amounts in EPS samples. Only small amounts of polysaccharides (over 10%) were found in most analyzed EPS fractions. However, polysaccharides were the major components in the EPS produced by cells grown on pyrite (irrespective of lifestyle) and glucose. They played a main role in adhesion, aggregation of bacterial cells, retention of water, adsorption of organic and inorganic compounds, binding of enzymes, as a nutrient source, and as a protective barrier to cells [3]. Polysaccharides represented up to approximately 55% of the total EPS composition in cells grown with glucose as the energy source. This finding agrees with the results obtained from zeta-potential measurements, where the obtained IEP values suggested an important presence of negatively charged polysaccharides on the surface of cells cultured with glucose. Glucose has been shown to be an efficient substrate for polysaccharide production, as it is readily assimilated by cells and used as a carbon and energy source. In contrast, other substrates such as tetrathionate, yeast extract, or ferrous iron could be less efficient for polysaccharide production, because they may require more complex metabolic pathways for assimilation and utilization [59,60]. Therefore, the amount and type of polysaccharides present in *A. copahuensis* EPS could be influenced by the nature and amounts of substrates available in the culture medium. *A. copahuensis* cells grown in

the presence of glucose showed an elevated tendency to form aggregates (Figure 1d). Cells could be using part of the supplemented energy source for the synthesis of extracellular polysaccharides, which contribute to stick cells. Barreto and colleagues [61] suggested that *At. ferrooxidans* can incorporate sugar monomers for the synthesize of exopolysaccharides. Studies carried out with *At. ferrooxidans* and *Ferroplasma acidiphilum* confirmed that the external addition of sugars such as glucose or galactose to the culture medium stimulate the production of capsular polysaccharides (CPS) [50,62]. Also, induction of extracellular polysaccharide secretion was registered in *At. Ferrooxidans*, *Haloarcula*, *Haloferax*, *Halococcus*, *Natronococcus*, *Halobacterium*, and *Sulfolobus* species [63,64]. However, glucose induced production of extracellular polysaccharides but did not lead to increase in the attachment of *A. copahuensis* cells to mineral surfaces [9,10].

In order to obtain information about the polysaccharides of *A. copahuensis*, FLBA was done. A total of 9 lectins were tested (Table 3). Two lectins, ConA and PWM, bound to glycoconjugates on the surface of *A. copahuensis* cells regardless of the growth condition. While the lectin ECA did not recognize glycoconjugates on *A. copahuensis* cells, the lectins PNA, SBA, LCH, UEA I, BS I, and PHA-E bound deferentially to the cell surfaces depending on the state and growth conditions of the cells. These results showed that *A. copahuensis* produced different glycoconjugates according to the culture condition and the state of the cells. A major diversity of glycoconjugates and stronger lectin signal were found in sessile cells as compared with planktonic cells.

Table 3. Fluorescence lectin binding assays (FLBA).

Lectin	Specificities	Growth Condition			
		S° + YE	Fe + YE	FeS$_2$	
		Planktonic	Planktonic	Planktonic	Sessile
ConA	D(+)glucose; D(+)mannose	+	+	+	+
PNA	D(+)galactose	+	-	-	+
LcH	α-mannose; α-glucose	-	+	+	+
WGA	*N*-acetyl-glucosamine	-	-	-	+
ECA	*N*-acetyl-D-galactosamine; D-galactose	-	-	-	-
SBA	α- and β-*N*-acetylgalactosamine	x	+	-	+
UEA I	L(-)fucose	-	+	+	+
PWM	*N*-acetyl-glucosamine	+	+	+	+
BS I	α-D-galactosyl; *N*-acetyl-α-D-galactosaminyl	-	+	-	+
PHA-E	galactose	-	+	+	+

+: lectin positive; -: no signals found; x: not tested.

Previous confocal laser scanning microcopy (CLSM) studies combined with strain-specific fluorescently labeled lectins have allowed the identification of single species on binary biofilms of *S. metallicus* and *A. copahuensis* [6]. The expression of different glycoconjugates was also observed for a closely related strain *Acidianus* sp. DSM 29099 [65]. These results confirm that the expression of glycoconjugates is substrate- and cell stage-dependent; it also varies between species and even between related strains.

The lectin binding results revealed the presence of carbohydrates containing glucose, mannose, galactose, fucose, *N*-acetylgalactosamine, and *N*-acetylglucosamine residues on *A. copahuensis* cell surfaces. These residues were predominant in the EPS of *Thermococcus litoralis*, *Sulfolobus* species, and haloarchaeal biofilms [19,66]. Archaeal *N*-glycans are highly diverse and composed of a variety of different sugar residues, such as glucose, mannose, rhamnose, glucuronic acid, iduronic acid, *N*-acetylgalactosamine, *N*-acetylglucosamine, galactofuranose, sulfoquinovose, and galactouronic acid [67]. Some of the tested lectins likely bound to *N*-glycanes presents in the S-layer. Glycosylation represents the most frequent modification of S-layer proteins; it constitutes a remarkable characteristic of many archaeal S-layer proteins [68]. *N*-glycosylation may contribute to the ability of Archaea and

their proteins to survive or adapt to the harsh environments in which these organisms can thrive [67].

Functional groups of EPS were explored by FTIR analyses (Figure 4). The FTIR spectra of EPS from *A. copahuensis* showed similar characteristics (Supplementary Materials, Figure S1). A broad band was registered at ~3.400 cm^{-1}, attributed to stretching vibration of the hydroxyl functional group into polymeric compounds and N-H stretching vibrations in amides and amines. The band at 2830 cm^{-1} in the spectra of EPS extracted from glucose-grown cells corresponded to C-H stretching vibrations in the hydrocarbon chains. The picks around 1650 cm^{-1} were assigned to C-N and C=O stretching vibration of β-sheets in secondary protein structures. The band at 1536 cm^{-1} in EPS extracted from yeast extract–grown cells (Figure S1) may be associated with amide II due to a combination of the bending N-H of amides and the contributions from the stretching C-N groups. The bands at ~1380 cm^{-1} are mainly from symmetric stretching vibrations of the COO-group in carboxylate anions and due to asymmetric and symmetric deformations of methyl groups. The abundances of polysaccharides and phosphorylated compounds were indicated by vibrations at ~1150 cm^{-1} and 1070 cm^{-1}, respectively. The region < 1000 cm^{-1} was assigned to the presence of phosphate and sulfur functional groups.
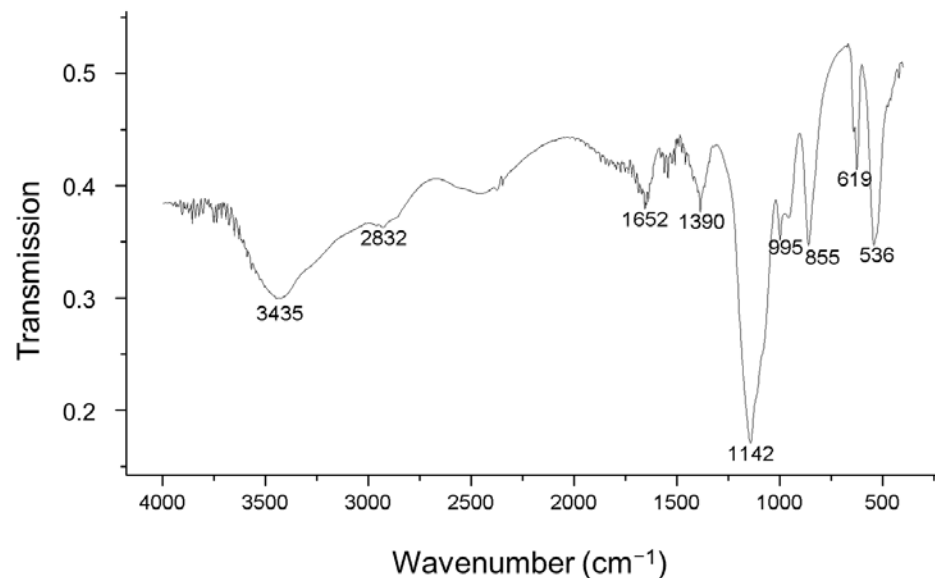

Figure 4. Representative FTIR spectrum of EPS produced by *A. copahuensis* cells grown with glucose.

The FTIR spectra clearly indicate the presence of carbon, phosphorus, and nitrogen in the EPS produced by *A. copahuensis*. FTIR signals varied subtlety with energy sources. These indicate that functional group composition on the surface of *A. copahuensis* was not sensitive to the available energy sources. These results confirm that the differences between IEPs of cells cultured with different substrates are more related to the amounts rather than the kind of functional groups presented on the *A. copahuensis* cell surface.

3.4. Pyrite Leaching

Figure 5 shows the total iron concentrations after 10 days of bioleaching of pyrite by *A. copahuensis*. The oxidative activity of *A. copahuensis* cells adapted to grow on different substrates was monitored by measuring pH and iron concentration in solution. Most of the iron measured was in the form of iron(III). In all conditions, the iron(II) concentration remained constant and very low (approximately 6 ppm) throughout the experiment. In the abiotic control, only 12 ppm of total iron was solubilized at the end of the experiment. When cells were previously grown on glucose, sulfur, or tetrathionate and yeast extract, the total iron concentrations were 92 ppm, 123 ppm, and 80 ppm, respectively. In flasks inoculated with cells previously grown on pyrite, the concentration of total iron in solution reached

approximately 4500 ppm after 10 days of incubation. Cells adapted to grow on pyrite showed increased oxidative activity on pyrite accompanied by increased production of capsular EPS. These results are in agreement with previous observations in which a higher affinity for adhesion and biofilm formation on pyrite were detected when *A. copahuensis* cells were adapted to grow on pyrite [69].
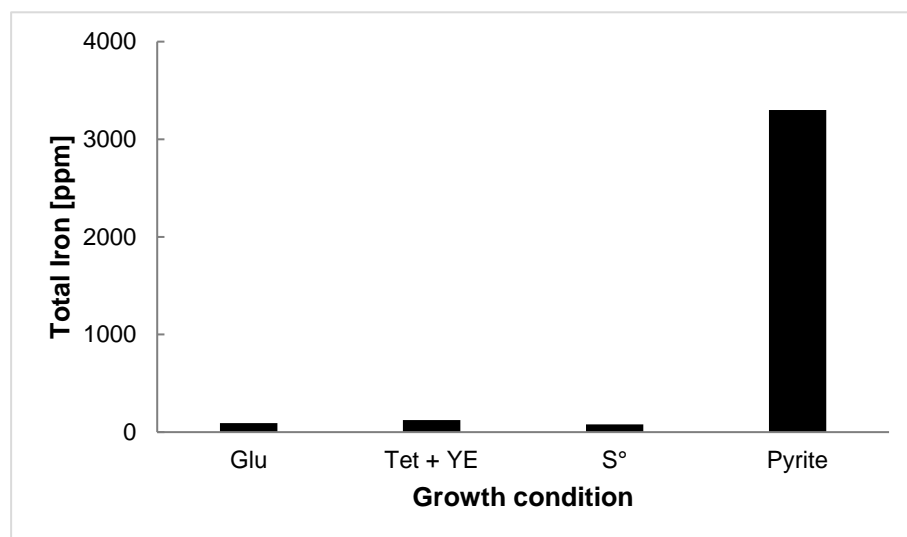

Figure 5. Bioleaching of pyrite by *A. copahuensis* cells pre-grown with glucose, tetrathionate and yeast extracts, sulfur, or pyrite after 10 days of cultivation.

4. Conclusions

According to the obtained results, the cell surface characteristics of *A. copahuensis* were dependent on the cultivation conditions. Non-soluble substrates induced changes on cell surface structures, including the presence of cell appendages, wider cell envelopes, higher hydrophobicities, and larger EPS production, compared with cells grown with soluble substrates. These results suggest that physical contact, including hydrophobic and electrostatic interactions between the cell and mineral surface, could be involved in cell adhesion to pyrite and sulfur. EPS analysis revealed variable proportions of polysaccharides, proteins, uronic acids, and humic-like substances. Carbohydrates mainly included glucose, mannose, galactose, fucose, *N*-acetylgalactosamine, and *N*-acetylglucosamine residues, suggesting that *N*-glycosylation is involved in the functionality and stability of the cell surface structure. EPS has been shown to be important for the adhesion of *A. copahuensis* cells to the pyrite surface and possibly to other minerals, which has important implications for mineral bioleaching. Therefore, understanding the mechanisms of EPS production and composition may be important for improving mineral bioleaching processes.

References

1. Kaksonen, A.H.; Boxall, N.J.; Gumulya, Y.; Khaleque, H.N.; Morris, C.; Bohu, T.; Cheng, K.Y.; Usher, K.M.; Lakaniemi, A.M. Recent Progress in Biohydrometallurgy and Microbial Characterisation. *Hydrometallurgy* **2018**, *180*, 7–25. [CrossRef]
2. Sand, W.; Schippers, A.; Hedrich, S.; Vera, M. Progress in Bioleaching: Fundamentals and Mechanisms of Microbial Metal Sulfide Oxidation–Part A. *Appl. Microbiol. Biotechnol.* **2022**, *106*, 6933–6952. [CrossRef]
3. More, T.T.; Yadav, J.S.S.; Yan, S.; Tyagi, R.D.; Surampalli, R.Y. Extracellular Polymeric Substances of Bacteria and Their Potential Environmental Applications. *J. Environ. Manag.* **2014**, *144*, 1–25. [CrossRef] [PubMed]
4. Castro, C.; Urbieta, M.S.; Plaza Cazón, J.; Donati, E.R. Metal Biorecovery and Bioremediation: Whether or Not Thermophilic Are Better than Mesophilic Microorganisms. *Bioresour. Technol.* **2019**, *279*, 317–326. [CrossRef] [PubMed]
5. He, Z.; Yang, Y.; Zhou, S.; Zhong, H.; Sun, W. The Effect of Culture Condition and Ionic Strength on Proton Adsorption at the Surface of the Extreme Thermophile *Acidianus Manzaensis*. *Colloids Surf. B Biointerfaces* **2013**, *102*, 667–673. [CrossRef] [PubMed]
6. Castro, C.; Zhang, R.; Liu, J.; Bellenberg, S.; Neu, T.R.; Donati, E.; Sand, W.; Vera, M. Biofilm Formation and Interspecies Interactions in Mixed Cultures of Thermo-Acidophilic Archaea *Acidianus Spp.* and *Sulfolobus metallicus*. *Res. Microbiol.* **2016**, *167*, 604–612. [CrossRef] [PubMed]
7. Giaveno, M.A.; Urbieta, M.S.; Ulloa, J.R.; González Toril, E.; Donati, E.R. Physiologic Versatility and Growth Flexibility as the Main Characteristics of a Novel Thermoacidophilic *Acidianus* Strain Isolated from Copahue Geothermal Area in Argentina. *Microb. Ecol.* **2012**, *65*, 336–346. [CrossRef]
8. Sofía Urbieta, M.; Rascovan, N.; Vázquez, M.P.; Donati, E. Genome Analysis of the Thermoacidophilic Archaeon *Acidianus Copahuensis* Focusing on the Metabolisms Associated to Biomining Activities. *BMC Genom.* **2017**, *18*, 1–14. [CrossRef]
9. Castro, C.; Donati, E.R. Improving Zinc Recovery by Thermoacidophilic Archaeon *Acidianus Copahuensis* Using Tetrathionate. *Trans. Nonferrous Met. Soc. China* **2016**, *26*, 3004–3014. [CrossRef]
10. Castro, C.; Donati, E. Effects of Different Energy Sources on Cell Adhesion and Bioleaching of a Chalcopyrite Concentrate by Extremophilic Archaeon *Acidianus Copahuensis*. *Hydrometallurgy* **2016**, *162*, 49–56. [CrossRef]
11. Safar, C.; Castro, C.; Donati, E. Importance of Initial Interfacial Steps during Chalcopyrite Bioleaching by a Thermoacidophilic Archaeon. *Microorganisms* **2020**, *8*, 1009. [CrossRef] [PubMed]
12. Mackintosh, M.E. Nitrogen Fixation by Thiobacillus Ferrooxidans. *J. Gen. Microbiol.* **1978**, *105*, 215–218. [CrossRef]
13. Li, Q.; Sand, W. Mechanical and Chemical Studies on EPS from *Sulfobacillus Thermosulfidooxidans*: From Planktonic to Biofilm Cells. *Colloids Surf. B Biointerfaces* **2017**, *153*, 34–40. [CrossRef]
14. Dubois, M.; Gilles, K.A.; Hamilton, J.K.; Rebers, P.A.; Smith, F. Colorimetric Method for Determination of Sugars and Related Substances. *Anal. Chem.* **1956**, *28*, 350–356. [CrossRef]
15. Bradford, M.M. A Rapid and Sensitive Method for the Quantitation of Microgram Quantities of Protein Utilizing the Principle of Protein-Dye Binding. *Anal. Biochem.* **1976**, *72*, 248–254. [CrossRef] [PubMed]
16. Blumenkrantz, N.; Asboe-Hansen, G. New Method for Quantitative Determination of Uronic Acids. *Anal. Biochem.* **1973**, *54*, 484–489. [CrossRef] [PubMed]
17. Frølund, B.; Suci, P.A.; Langille, S.; Weiner, R.M.; Geesey, G.G. Influence of Protein Conditioning Films on Binding of a Bacterial Polysaccharide Adhesin from *Hyphomonas* MHS-3. *Biofouling* **1996**, *10*, 17–30. [CrossRef] [PubMed]
18. Caldwell, D.H.; Adams, R.B. Colorimetric Determination of Iron in Water With O-Phenanthroline. *J. Am. Water Work. Assoc.* **1946**, *38*, 727–730. [CrossRef]
19. Remonsellez, F.; Orell, A.; Jerez, C.A. Copper Tolerance of the Thermoacidophilic Archaeon *Sulfolobus Metallicus*: Possible Role of Polyphosphate Metabolism. *Microbiology* **2006**, *152*, 59–66. [CrossRef]
20. Paula, F.S.; Chin, J.P.; Schnürer, A.; Müller, B.; Manesiotis, P.; Waters, N.; Macintosh, K.A.; Quinn, J.P.; Connolly, J.; Abram, F.; et al. The Potential for Polyphosphate Metabolism in Archaea and Anaerobic Polyphosphate Formation in Methanosarcina Mazei. *Sci. Rep.* **2019**, *9*, 1–12. [CrossRef]
21. Toso, D.B.; Javed, M.M.; Czornyj, E.; Gunsalus, R.P.; Hong Zhou, Z.; Zhou, H. Discovery and Characterization of Iron Sulfide and Polyphosphate Bodies Coexisting in *Archaeoglobus Fulgidus* Cells. *Archaea* **2016**, *2016*, 4706532. [CrossRef]
22. Wang, L.; Liu, Q.; Wu, X.; Huang, Y.; Wise, M.J.; Liu, Z.; Wang, W.; Hu, J.; Wang, C. Bioinformatics Analysis of Metabolism Pathways of Archaeal Energy Reserves OPEN. *Sci. Rep.* **2019**, *9*, 1034. [CrossRef] [PubMed]
23. Gorlas, A.; Marguet, E.; Gill, S.; Geslin, C.; Guigner, J.-M.; Guyot, F.; Forterre, P. Sulfur Vesicles from Thermococcales: A Possible Role in Sulfur Detoxifying Mechanisms. *Biochimie* **2015**, *118*, 356–364. [CrossRef] [PubMed]
24. Dahl, C.; Prange, A. Bacterial Sulfur Globules: Occurrence, Structure and Metabolism. In *Inclusions in Prokaryotes*; Springer-Verlag: Berlin/Heidelberg, Germany, 2006; pp. 21–51.
25. Franz, B.; Lichtenberg, H.; Hormes, J.; Modrow, H.; Dahl, C.; Prange, A. Utilization of Solid "elemental" Sulfur by the Phototrophic Purple Sulfur Bacterium Allochromatium Vinosum: A Sulfur K-Edge X-Ray Absorption Spectroscopy Study. *Microbiology* **2007**, *153*, 1268–1274. [CrossRef] [PubMed]
26. Eichinger, I.; Schmitz-Esser, S.; Schmid, M.; Fisher, C.R.; Bright, M. Symbiont-Driven Sulfur Crystal Formation in a Thiotrophic Symbiosis from Deep-Sea Hydrocarbon Seeps. *Environ. Microbiol. Rep.* **2014**, *6*, 364–372. [CrossRef] [PubMed]
27. Jarrell, K.F.; Albers, S.-V.; Nuno De Sousa Machado, J. A Comprehensive History of Motility and Archaellation in Archaea. *FEMS Microbes* **2021**, *2*, 2. [CrossRef]

28. Albers, S.-V.; Jarrell, K.F. The Archaellum: An Update on the Unique Archaeal Motility Structure. *Trends Microbiol.* **2018**, *26*, 351–362. [CrossRef]

29. Ng, S.Y.M.; Zolghadr, B.; Driessen, A.J.M.; Albers, S.-V.; Jarrell, K.F. Cell Surface Structures of Archaea. *J. Bacteriol.* **2008**, *190*, 6039–6047. [CrossRef]

30. Albers, S.-V.; Meyer, B.H. The Archaeal Cell Envelope. *Nat. Rev. Microbiol.* **2011**, *9*, 414–426. [CrossRef]

31. Wheaton, G.; Counts, J.; Mukherjee, A.; Kruh, J.; Kelly, R. The Confluence of Heavy Metal Biooxidation and Heavy Metal Resistance: Implications for Bioleaching by Extreme Thermoacidophiles. *Minerals* **2015**, *5*, 397–451. [CrossRef]

32. Zolghadr, B.; Klingl, A.; Koerdt, A.; Driessen, A.J.M.; Rachel, R.; Albers, S.-V. Appendage-Mediated Surface Adherence of *Sulfolobus Solfataricus*. *J. Bacteriol.* **2010**, *192*, 104–110. [CrossRef]

33. Bromfield, L.; Africa, C.-J.; Harrison, S.T.L.; van Hille, R.P. The Effect of Temperature and Culture History on the Attachment of *Metallosphaera Hakonensis* to Mineral Sulfides with Application to Heap Bioleaching. *Miner. Eng.* **2011**, *24*, 1157–1165. [CrossRef]

34. He, H.; Yang, Y.; Xia, J.; Ding, J.; Zhao, X.; Nie, Z. Growth and Surface Properties of New Thermoacidophilic Archaea Strain *Acidianus Manzaensis* YN-25 Grown on Different Substrates. *Trans. Nonferrous Met. Soc. China* **2008**, *18*, 1374–1378. [CrossRef]

35. Zhang, R.; Neu, T.R.; Blanchard, V.; Vera, M.; Sand, W. Biofilm Dynamics and EPS Production of a Thermoacidophilic Bioleaching Archaeon. *New Biotechnol.* **2019**, *51*, 21–30. [CrossRef] [PubMed]

36. Ehrlich, H.L.; Newman, D.K.; Kappler, A. *Geomicrobiology*, 4th ed.; M. Dekker: New York, NY, USA, 2002; ISBN 0824707648.

37. Ohmura, N.; Kitamura, K.; Saiki, H. Selective Adhesion of *Thiobacillus Ferrooxidans* to Pyrite. *Appl. Environ. Microbiol.* **1993**, *59*, 4050. [CrossRef] [PubMed]

38. Bellenberg, S.; Huynh, D.; Poetsch, A.; Sand, W.; Vera, M. Proteomics Reveal Enhanced Oxidative Stress Responses and Metabolic Adaptation in *Acidithiobacillus Ferrooxidans* Biofilm Cells on Pyrite. *Front. Microbiol.* **2019**, *10*, 592. [CrossRef]

39. Camacho, D.; Frazao, R.; Fouillen, A.; Nanci, A.; Lang, B.F.; Apte, S.C.; Baron, C.; Warren, L.A. New Insights Into *Acidithiobacillus Thiooxidans* Sulfur Metabolism Through Coupled Gene Expression, Solution Chemistry, Microscopy, and Spectroscopy Analyses. *Front. Microbiol.* **2020**, *11*, 411. [CrossRef]

40. Yin, L.; Yang, H.Y.; Lu, L.S.; Sand, W.; Tong, L.L.; Chen, G.B.; Zhao, M.M. miao Interfacial Alteration of Pyrite Caused by Bioleaching. *Hydrometallurgy* **2020**, *195*, 105356. [CrossRef]

41. Devasia, P.; Natarajan, K.A.; Sathyanarayana, D.N.; Rao, G.R. Surface Chemistry of *Thiobacillus Ferrooxidans* Relevant to Adhesion on Mineral Surfaces. *Appl. Environ. Microbiol.* **1993**, *59*, 4051–4055. [CrossRef]

42. Natarajan, K.A.; Das, A. Surface Chemical Studies on '*Acidithiobacillus*' Group of Bacteria with Reference to Mineral Flocculation. *Int. J. Miner. Process.* **2003**, *72*, 189–198. [CrossRef]

43. Chen, M.; Zhang, L.; Gu, G.; Hu, Y.; Su, L. Effects of Microorganisms on Surface Properties of Chalcopyrite and Bioleaching. *Trans. Nonferrous Met. Soc. China* **2008**, *18*, 1421–1426. [CrossRef]

44. Liu, H.; Gu, G.; Xu, Y. Surface Properties of Pyrite in the Course of Bioleaching by Pure Culture of Acidithiobacillus Ferrooxidans and a Mixed Culture of *Acidithiobacillus Ferrooxidans* and *Acidithiobacillus Thiooxidans*. *Hydrometallurgy* **2011**, *108*, 143–148. [CrossRef]

45. Sharma, P.; Das, A.; Hanumantha Rao, K.; Forssberg, K.S. Surface Characterization of Acidithiobacillus Ferrooxidans Cells Grown under Different Conditions. *Hydrometallurgy* **2003**, *71*, 285–292. [CrossRef]

46. Weerasooriya, R.; Tobschall, H.J. Pyrite–Water Interactions: Effects of PH and PFe on Surface Charge. *Colloids Surf. A Physicochem. Eng. Asp.* **2005**, *264*, 68–74. [CrossRef]

47. Paredes, A.; Acuña, S.M.; Gutiérrez, L.; Toledo, P.G. Zeta Potential of Pyrite Particles in Concentrated Solutions of Monovalent Seawater Electrolytes and Amyl Xanthate. *Minerals* **2019**, *9*, 584. [CrossRef]

48. Rijnaarts, H.H.M.; Norde, W.; Lyklema, J.; Zehnder, A.J.B. The Isoelectric Point of Bacteria as an Indicator for the Presence of Cell Surface Polymers That Inhibit Adhesion. *Colloids Surf. B Biointerfaces* **1995**, *4*, 191–197. [CrossRef]

49. Zhang, R.; Neu, T.R.; Li, Q.; Blanchard, V.; Zhang, Y.; Schippers, A.; Sand, W. Insight into Interactions of Thermoacidophilic Archaea with Elemental Sulfur: Biofilm Dynamics and EPS Analysis. *Front. Microbiol.* **2019**, *10*, 896. [CrossRef] [PubMed]

50. Bellenberg, S.; Leon-Morales, C.-F.; Sand, W.; Vera, M. Visualization of Capsular Polysaccharide Induction in *Acidithiobacillus Ferrooxidans*. *Hydrometallurgy* **2012**, *129–130*, 82–89. [CrossRef]

51. He, Z.; Yang, Y.; Zhou, S.; Hu, Y.; Zhong, H. Effect of Pyrite, Elemental Sulfur and Ferrous Ions on EPS Production by Metal Sulfide Bioleaching Microbes. *Trans. Nonferrous Met. Soc. China* **2014**, *24*, 1171–1178. [CrossRef]

52. Tourney, J.; Ngwenya, B.T. The Role of Bacterial Extracellular Polymeric Substances in Geomicrobiology. *Chem. Geol.* **2014**, *386*, 115–132. [CrossRef]

53. Yu, R.L.; Ou, Y.; Tan, J.X.; Wu, F.D.; Sun, J.; Miao, L.; Zhong, D.L. Effect of EPS on Adhesion of *Acidithiobacillus Ferrooxidans* on Chalcopyrite and Pyrite Mineral Surfaces. *Trans. Nonferrous Met. Soc. China* **2011**, *21*, 407–412. [CrossRef]

54. Govender, Y.; Gericke, M. Extracellular Polymeric Substances (EPS) from Bioleaching Systems and Its Application in Bioflotation. *Miner. Eng.* **2011**, *24*, 1122–1127. [CrossRef]

55. Rondel, C.; Marcato-Romain, C.-E.; Girbal-Neuhauser, E. Development and Validation of a Colorimetric Assay for Simultaneous Quantification of Neutral and Uronic Sugars. *Water Res.* **2013**, *47*, 2901–2908. [CrossRef] [PubMed]

56. Seviour, T.; Lambert, L.K.; Pijuan, M.; Yuan, Z. Structural Determination of a Key Exopolysaccharide in Mixed Culture Aerobic Sludge Granules Using NMR Spectroscopy. *Environ. Sci. Technol.* **2010**, *44*, 8964–8970. [CrossRef]

57. Flemming, H.-C.; Wingender, J. The Biofilm Matrix. *Nat. Rev. Microbiol.* **2010**, *8*, 623–633. [CrossRef]

58. Shi, Y.; Huang, J.; Zeng, G.; Gu, Y.; Chen, Y.; Hu, Y.; Tang, B.; Zhou, J.; Yang, Y.; Shi, L. Exploiting Extracellular Polymeric Substances (EPS) Controlling Strategies for Performance Enhancement of Biological Wastewater Treatments: An Overview. *Chemosphere* **2017**, *180*, 396–411. [CrossRef]

59. Barrie Johnson, D.; Hallberg, K.B. Carbon, Iron and Sulfur Metabolism in Acidophilic Micro-Organisms. *Adv. Microb. Physiol.* **2008**, *54*, 201–255. [CrossRef]

60. Liu, L.J.; Jiang, Z.; Wang, P.; Qin, Y.L.; Xu, W.; Wang, Y.; Liu, S.J.; Jiang, C.Y. Physiology, Taxonomy, and Sulfur Metabolism of the Sulfolobales, an Order of Thermoacidophilic Archaea. *Front. Microbiol.* **2021**, *12*, 3096. [CrossRef]

61. Barreto, M.; Jedlicki, E.; Holmes, D.S. Identification of a Gene Cluster for the Formation of Extracellular Polysaccharide Precursors in the Chemolithoautotroph *Acidithiobacillus Ferrooxidans*. *Appl. Environ. Microbiol.* **2005**, *71*, 2902–2909. [CrossRef]

62. Zhang, R.; Bellenberg, S.; Castro, L.; Neu, T.R.; Sand, W.; Vera, M. Colonization and Biofilm Formation of the Extremely Acidophilic Archaeon *Ferroplasma Acidiphilum*. *Hydrometallurgy* **2014**, *150*, 245–252. [CrossRef]

63. Orell, A.; Fröls, S.; Albers, S.-V. Archaeal Biofilms: The Great Unexplored. *Annu. Rev. Microbiol.* **2013**, *67*, 337–354. [CrossRef] [PubMed]

64. Saavedra, A.; Aguirre, P.; Gentina, J.C. Biooxidation of Iron by *Acidithiobacillus Ferrooxidans* in the Presence of D-Galactose: Understanding Its Influence on the Production of EPS and Cell Tolerance to High Concentrations of Iron. *Front. Microbiol.* **2020**, *11*, 759. [CrossRef] [PubMed]

65. Zhang, R.; Neu, T.R.; Zhang, Y.; Bellenberg, S.; Kuhlicke, U.; Li, Q.; Sand, W.; Vera, M. Visualization and Analysis of EPS Glycoconjugates of the Thermoacidophilic Archaeon *Sulfolobus metallicus*. *Appl. Microbiol. Biotechnol.* **2015**, *99*, 7343–7356. [CrossRef] [PubMed]

66. Fröls, S. Archaeal Biofilms: Widespread and Complex. *Biochem. Soc. Trans.* **2013**, *41*, 393–398. [CrossRef]

67. Meyer, B.H.; Albers, S.-V. Hot and Sweet: Protein Glycosylation in Crenarchaeota. *Biochem. Soc. Trans.* **2013**, *41*, 384–392. [CrossRef]

68. Zhu, C.; Guo, G.; Ma, Q.; Zhang, F.; Ma, F.; Liu, J.; Xiao, D.; Yang, X.; Sun, M. Diversity in S-Layers. *Prog. Biophys. Mol. Biol.* **2017**, *123*, 1–15. [CrossRef]

69. Castro, C.; Vera, M.; Donati, E.; Sand, W. Visualization of Attachment and Colonization of Pyrite Surfaces by a Novel Species of *Acidianus*. In *Advanced Materials Research*; Trans Tech Publications Ltd.: Wollerau, Switzerland, 2013; Volume 825, ISBN 9783037858912.